The Use of iPad LiDAR to Build a Digital Elevation Model in Defining Customary Zones (Case Study of Panglipuran, Bali)

Asep Yusup Saptari[1], Ratri Widyastuti[1], Ketut Tomy Suhari[2], Afnan Dwi Suseno[1], Andri Hernandi[1], Rizqi Abdul Haris[1], Sella Lestari Nurmaulia[1]

[1]Institut Teknologi Bandung (ITB), Geodesy and Geomatics, Earth Science and Technology Faculty, Indonesia
[2] Institut Teknologi Nasional (ITN) Malang, Indonesia

Keywords: LiDAR, iPad, Point Clouds, Customary, Georeference

Abstract

The LiDAR on the iPad device can be used for surveying and mapping. However, the accuracy and precision of the LiDAR scanner on the iPad are not as high as the LiDAR system on Terrestrial Laser Scanning (TLS), with a more limited range and smaller coverage area. Still, the LiDAR sensor integrated into the iPad has advantages when compared to professional LiDAR systems, including the iPad LiDAR as a low-cost portable 3D scanner, dynamic portability, speed, easy use at close range so that it can be used to scan objects with high density and can reach areas/parts of objects that are difficult to be covered by TLS. The 3D modelling method using iPad LiDAR is a solution for building 3D models.
Since iPad's point cloud data is not integrated with the global coordinate system, a georeferencing process is necessary to produce DEM (Digital Elevation Model), which will be used to define customary zones in Panglipuran Heritage Village. The georeferencing process is carried out by transforming the iPad's LiDAR coordinates system to the global reference coordinates resulting from GNSS measurements. The scanning strategy must be well arranged. In addition, good control point design determines the quality of control point transformation results into a global reference coordinate system.
This research contributes to obtaining an alternative low-cost 3D mapping method for cultural conservation areas using LiDAR technologies. This method is inexpensive but still considers geospatial quality aspects so it can be used for the decision-making process in spatial planning of cultural regions.

1. Introduction

Penglipuran customary village is in Bangli District, Bangli Regency, Bali Province. Penglipuran has a distinctive spatial pattern based on the Tri Hita Karana concept, which consists of three connecting elements between nature and humans to achieve the perfection of life, soul, body and energy, which involves the harmony of human relations with the creator, fellow humans and nature to create three sources of happiness. (Sudarwani, 2018). Tri Hita Karana concept is used as the philosophical basis for determining the spatial value of the Hindu-Balinese community, which emphasizes the balance of relationships in the context of harmony and compatibility between humans, the environment and God, which is manifested in the scale of residential space (Arimbawa et al., 2017). According to this concept, the spatial layout of Penglipuran Traditional Village is divided into 3 zones: utama mandala zone, madya mandala zone and nista mandala zone. (Ariesta et al., 2021). The zones have different characteristics of customs and cultures. In addition, between one customary zone and another, there are unique spatial patterns.
Spatial patterns are used to identify each customary zone in Penglipuran Traditional Village. This spatial pattern can be seen from topographic data, including the Digital Elevation Model (DEM), which shows the height level of an observed location. Several 3D/DEM mapping techniques are developing rapidly through photogrammetry and Light Detection and Ranging (LiDAR) methods. LiDAR transmission can carried out through several platforms, including air platforms known as Airborne Laser Scanning (ALS) and terrestrial platforms known as Terrestrial Laser Scanner (TLS) (Vosselmann and Mass, 2010). Both LiDAR and TLS methods have their advantages and disadvantages. LiDAR technology is not static; it has also developed into dynamic technology. One of them is the Handheld Laser Scanner (HLS). TLS cannot capture some parts of the object due to the limited field of view because TLS is a static laser instrument. HLS can be a complement that can scan objects in detail in areas TLS cannot reach. Both of these technologies can scan objects accurately to fractions of a mm, with the output being a collection of point data that forms an object called a point cloud (Saptari et al., 2022).

In further developments, LiDAR technology has been dynamically integrated into the iPad hardware. LiDAR technology on the iPad enables augmented reality creation and better-quality portrait effects. LiDAR on iPad devices also has the potential to be used for mapping and surveying. However, the accuracy and precision of LiDAR scanners on iPads are not as high as those of static LiDAR systems on TLS and ALS. The LiDAR sensor integrated into the iPad has advantages, including cost-effectiveness, portability, speed, and ease of use at close range (Spreafico et al., 2021).

In this study, data acquisition and 3D modelling were completed using the LiDAR sensor on the iPad Pro M1 2021 device. The results of the LiDAR method acquisition in the form of point cloud data from observed objects will be georeferenced using Ground Control Point (GCP) and Independent Check Point (ICP) data. Georeferenced point clouds are processed into DEMs (Digital Elevation Models) and used to define customary zones in Penglipuran village. As a comparison of output, this study also compares 3D visualisation obtained from iPad Pro M1 2021 LiDAR data against 3D visualisation from the photogrammetry method and the existing TLS (Terrestrial Laser Scanner) method. The differences in the visualisation results of the three data can be assessed by comparing these three methods. The data on the

characteristics of each customary zone were obtained from the interview method and literature study in the next stage; the final product can be built from the integration of the characteristics of each customary zone with DEM data.

2. Literature Review

The LiDAR sensor on the iPhone and iPad hardware has an accuracy of 5 mm range from the sensor with a point density of about 7225 dots/m2 at 25 cm. The density decreases with a range of 150 dots/m2 at an observation distance of 250 cm. (King et al. 2022). LiDAR sensors are used to create 3D visualisations that are considered accurate in the form of point clouds in a dense form. Point clouds are collected and combined to obtain spatial information in the form of x, y, and z coordinates of objects/targets. Data acquisition using LiDAR technology on Apple devices can be completed in two techniques: static and dynamic (Spreafico et al., 2021).

Several studies related to LiDAR sensors on iPad devices implementation have been carried out, such as those performed by Gursel et al (2021) using LiDAR sensors for accurate and fast analysis of diameter at breast height (DBH). Labed´z (2022) has also performed a quality analysis of 3D models from iPad LiDAR data. The most common errors are geometric multiplication and incorrect merging of adjacent model fragments. Regarding development, the iPad LiDAR device is a low-cost solution compared to TLS. The software is related to mobile device applications for metric 3D observation using software on the iPad (Losè et al., 2022).

iPad LiDAR can be used to measure the perimeter at breast height (PBH) for urban forest inventory in a small community with a limited budget; this procedure can be done more independently and quickly using a simple device such as the iPad Pro even from a limited distance of between 1 to 2 meters. Convert tree point cloud coordinates from iPad Pro to georeferencing system using target sphere and reference coordinates from HLS (Bobrowski et al., 2022). For 3D observation purposes, “scan to BIM” iPad LiDAR showed promising results. The best distance from the iPad to the target is 1 to 1.5 meters. However, the maximum distance to the target is 5 meters, and iPad LiDAR observation is very suitable for indoor mapping (Teo et al., 2023).

In topographic measurement or mapping, the LiDAR sensor on the Apple iPad Pro 2020 can describe topography with an accuracy of up to several centimetres as well as measured using terrestrial laser scanning or GNSS survey equipment. To achieve these results, care and slowness are required when collecting the scan results to avoid 'biases'. iPad scans are not registered or oriented vertically correctly when exported. Therefore, an object or target with known coordinates (control points) must transform the scan to the proper orientation and position. (Nelson, 2022). The latest Apple iPad and iPhone Pro devices have applications for small to medium-scale morphological features, ranging from centimetres to several hundred meters in various earth science disciplines such as geomorphology, geology, forestry, and archaeology. iPad and iPhone sensors perform similarly, but the smaller size of the iPhone provides greater flexibility. Overall, the LiDAR sensors that are available for the iPad Pro and iPhone Pro models offer a new, cost-effective and time-efficient alternative to existing topographic survey methods such as TLS and Structure From Motion (SfM) Multi-View Stereo MVS, capable of quickly scanning small- to medium-scale landscape topography at high spatial resolution. However, the accuracy and precision of the iPhone LiDAR model do not yet reach the current SfM MVS standard (Luetzenburg, 2021).

iPad LiDAR cloud point coordinate system can be transformed into a global coordinate system by performing three-dimensional transformation. With its advanced technology, this sensor can measure distance, create 3D maps, and accurately detect objects in limited areas. This feature is handy for architecture, engineering, construction professionals, land surveyors, and geospatial analysts. However, it is essential to note that the accuracy of the LiDAR sensor can be affected by external factors such as lighting and weather conditions (Hakim, 2023). LiDAR data can be applied to a georeferenced system to help find objects in the scene globally. The global position of objects, such as vehicles and pedestrians (Senapati, 2020). Penglipuran Village, the object of this research, is located in Kubu Village, Bangli District, Bangli Regency, Bali Province. Penglipuran Village is one of the customary villages that are famous as tourist destinations in Bali because its people still preserve and practice local wisdom and traditional Balinese culture in their daily lives.

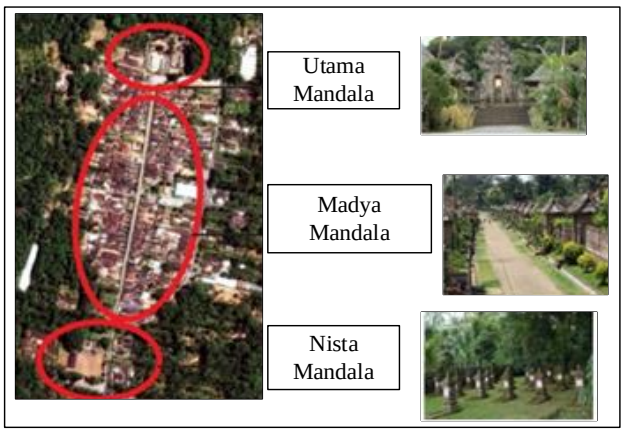

Figure 1. Definition of Customary Zones According to the Tri Angga Concept, which is Included in the Tri Hita Karana Concept (Source: Priyoga & Sudarwani, 2018)

These customary rules contain social norms and laws that apply to the lives of the Penglipuran Village community. In addition to local wisdom and traditional culture, Penglipuran Village is also famous for its well-preserved traditional Balinese architecture. The concept of spatial hierarchy, known as Tri Angga, is an essential element in the Tri Hita Karana Concept, which involves the division of the zone system in traditional Balinese architectural planning, which consists of three primary levels, namely the utama mandala zone, madya mandala, and nista mandala (Priyoga & Sudarwani, 2018)as illustrated in Figure 1. The division of the area aims to clarify the spatial planning and layout of buildings and social activities in Penglipuran Village.

3. Methods

3.1 LiDAR Data Acquisition

The LiDAR data acquisition process uses Dynamic Acquisition, which has the same working method as a Handheld Laser Scanner (HLS). Handheld Laser Scanner (HLS) visualizes 3-dimensional shapes through a triangulation mechanism. A laser/light point or lane is projected onto the object from the device, and the sensor measures the distance to the surface (Salleh et al., 2018). This scanning process is done by pointing the device at the target object. In the iPad hardware technology for the data acquisition process, the scanned point cloud is stored in local coordinates/instrument coordinates that have not been integrated into the global coordinate system so that to obtain coordinates in the global/earth system, a 3D transformation process is required to the earth system. Therefore, data acquisition activities include GNSS data acquisition and

scanning of the study area. In addition, data acquisition was also conducted by interviewing the 'Kliyan Adat' of Penglipuran village to obtain information on semantic data in the form of data on the division of customary zones along with their characteristics. The data acquisition process focuses on the area to be modelled only; the area to be modelled is the main road and two sample housing complexes.

3.2 Point Clouds Data Processing

Point cloud data processing is intended to obtain results in the form of feasible and reliable data in forming 3D models. Raw data point clouds are initially processed to produce georeferenced data in a global coordinate system. The data processing is carried out in several stages, including registration and filtering. The registration process is carried out using the cloud-to-cloud registration method with the Iterative Closest Point (ICP) algorithm in stages between point clouds. In this algorithm, correspondence is carried out from each point used as a common point between adjacent and overlapping point clouds by selecting objects that can be used as common points and identified from both overlapping scan results. Objects used as common points are natural objects that are the same and easily recognisable. In addition, these points can also be ICP and GCP points that have been measured using GPS. The minimum number of common points (ICP points) recommended is a minimum of four points (Jacobs, 2005) to have redundancy.

The filtering process on point clouds is critical to get accurate and quality results by eliminating noise in point cloud data. Noise in point clouds can be made up by various factors, such as moving objects during scanning, unwanted light reflections, or inaccuracies in the scanning device. By doing the filtering process, noise or unnecessary data can be removed so that the filtered point clouds are cleaner and more accurate. The filtering method used in this study is the fencing technique. The fencing technique in the point cloud filtering process separates the area from the area that will not be filtered (considered not to contain noise).

3.3 Georeferencing.

Georeferencing point clouds is the process of binding geographic locations to individual points that make up point cloud data. Georeferencing generally transforms point clouds from local coordinates to global sister coordinates. (Reshetyuk, 2009). The Georeferencing process seamlessly references point cloud data with a known coordinate or reference system. Several methods can be used to georeference point clouds. One common approach is to use GCPs or ICPs, identifiable features in point clouds with known geographic coordinates. Point clouds can be georeferenced by identifying points and referencing them to known geographic coordinates. Coordinate information of GCP or ICP control points is measured using static GNSS, and the data is processed using post-processing methods. This study uses Helmert's transformation to maintain object conformity or to remain conformal. Helmert transformation is often referred to as similarity transformation.

It is essential to design and plan the distribution of control points. In the planning survey, the distribution of GCP and ICP must be in accordance with the need for georeferencing iPad LiDAR point cloud data by considering the capabilities and limitations of the iPad Pro M1 2021 LiDAR and the needs of the objects to be modelled.

Figure 2. (a) Distribution of GCP in the observed area (customary zone). (b) Distribution of ICP in the observed area

GCP control point measurements were carried out using the Global National Satellite System (GNSS) Static Radial method using a Geodetic GPS tool. The GNSS Static Radial method is one of the most accurate and precise measurement techniques for determining the position of a point on the Earth's surface. This study measured six control points at the Penglipuran Traditional Village, Bali.

3.4 DEM Generation.

DEM is a digital/numerical representation of the Earth's elevation. Elevation is the height above a particular surface, such as sea level. Elevation emphasises the measurement from a reference point to the top of an object. It may contain the concept of height, but it also tries to include geographical elements and other natural features (Li, 2005). DEM generated in the study area represents the land surface or relief of the Earth without considering the presence of buildings or vegetation in the observed area.

4. Discussion And Result

4.1 Control Points and Scanning Design

The survey planning distribution of GCP and ICP framework points is designed with the aim of the number and accuracy according to needs. The framework's design affects the process of acquiring point cloud data using LiDAR iPad Pro M1 2021. The design of the control point network plans 6 GCP points measured using the GNSS radial static method and 30 ICP points using the GNSS RTK or Real-Time Kinematic method. By considering the shape and size of the object to be scanned, the scanning process is designed with nine lanes. The number of lanes is also adjusted to the capabilities of the LiDAR sensor on the iPad Pro M1 2021, which has limitations in scanning distance. The scan design also considers the visibility of GCP and ICP in the two overlapping scan results to obtain maximum registration results between point cloud data.

Based on the results of the planning survey, there are two GCP points in house zone number 5, namely GCPC and GCPD, two points in house zone number 3, namely GCPA and GCPB, and two GCPs in the temple area, namely GCPC_PURA and GCPD_PURA. Figure 3, the area with coloured polygon, shows that in house zone 3 and lane 4, there are only three control points for LiDAR scanning. This is because when planning house zone number 3, carrying out measurements was not a priority. Therefore, the number of control points was not evenly distributed in house zone number 3, where the LiDAR scanning of the iPad Pro M1 2021 was carried out. When looking at the scanning design, the scanning area is not evenly distributed due to the elevation factor and the variation of objects around the research area. The flatter the scanning area elevation and the fewer obstructing objects, the larger the scanning area will be.

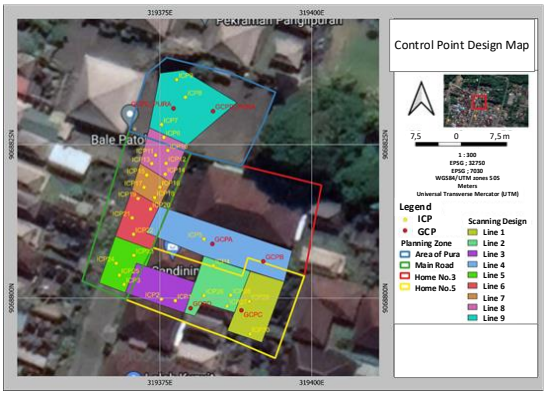

Figure 3. Control point planning design around the customary zone (coloured polygon)

4.2 Coordinate Measurement of Ground Control Point (GCP) and Independent Check Point (ICP) Results

The implementation of GCP measurements uses four geodetic receivers of the Stonex S800A and Stonex S9 types simultaneously with static mode. The GNSS receivers used are the types Stonex S9/STNS86391011, Stonex S800A / S813571202036, Stonex S800A / S813571202038, Stonex S800A / S813571202029. Stonex S9 has a horizontal accuracy of 2.5 mm ± 1 ppm Root Mean Square/RMS and a vertical accuracy of 5.0 mm ± 1 ppm RMS, and Stonex S800A has a horizontal accuracy of 2.5 mm ± 1 ppm RMS and a vertical accuracy of 5.0 mm ± 1 ppm RMS. This accuracy is perfect for conducting GNSS measurements with the radial static method. The GNSS measurement using the radial static method is processed using the post-processing method. In contrast, the measurement of the ICP points is carried out using the GNSS Real-Time Kinematic method.

GNSS measurements were carried out at night, which is expected to reduce interference from other signals from human activities around the measurement area and produce accurate and precise data because the study location is a tourist area. The height reference system used refers to the ellipsoid system. Based on the results obtained from the Geospatial Information Agency (BIG) page https://srgi.big.go.id, The geoid undulation value in the measurement area for all control points is the same 36,751 meters with a standard deviation of 0.216 meters, so the difference in geoid undulation around the study area can be ignored. Thus, a height system referring to an ellipsoid can be used.

4.3 IPad LiDAR Scanning

each targeted object, as shown in Figure 4. The scanning process is carried out by considering the previously determined GCP and ICP distribution design. In addition, the scanning process considers the inter-scanning process so that the overlap between two adjacent scanning sessions is at least 30 per cent. The scanned point cloud data is raw in e.57 data format for the entire research study area. The distance or length of one scan varies between 10 to 20 meters. Therefore, 12 lanes of point cloud scanning were generated to scan the whole study area, as in Table 1, which shows the data on the number of points resulting from scanning the entire research study area. The iPad scan results, divided into several lanes, are gradually combined in the registration process. Figure 5 shows the scan of building BGN5_A with BGN5_B on lane 1 and lane 2.

Figure 4. Point Clouds Data Acquisition Process Using iPad Pro M1 2021

In its implementation, the point cloud scanning process did not match the planning, which caused a change in the number of lanes. At the time of design, it was planned that there would only be nine scanning lanes; however, during the data acquisition process, there were 12 scanning lanes for the same area as in Table 1; there was an addition to lane 10 into several sub-lanes.

No	Name	Lanes	Point Number
1	BGN5_A	Lane 1	11.994.467
2	BGN5_B	Lane 2	11.993.482
3	BGNJLN_3	Lane 4, Lane 6	11.993.534
4	BGNJLN_5	Lane 5, Lane 3	4.313.329
5	BGN5_3	Lane 3, Lane 2, Lane 4	11.991.335
6	BGN5_C	Lane 3, Lane 2	10.489.416
7	JLN_A	Lane 5, Lane 6, Lane 7,Lane 8	11.993.292
8	JLN_B	Lane 10	11.955.448
9	JLN_C		11.993.381
10	JLN_D		6.162.101
11	JLN_E		10.501.203
12	JLN_F		11.990.677

Table 1. Jumlah Point Hasil Pemindaian iPad LiDAR Seluruh Data Point Clouds

The addition of lanes occurs because several scanning sessions do not overlap during the data acquisition process, so changing the scanning lane or shortening the scanning line into shorter lanes of 10 to 20 meters is necessary. The number of points in one lane is influenced by the area being scanned and the duration of the scan. The longer the scan in one lane, the more points will be collected.

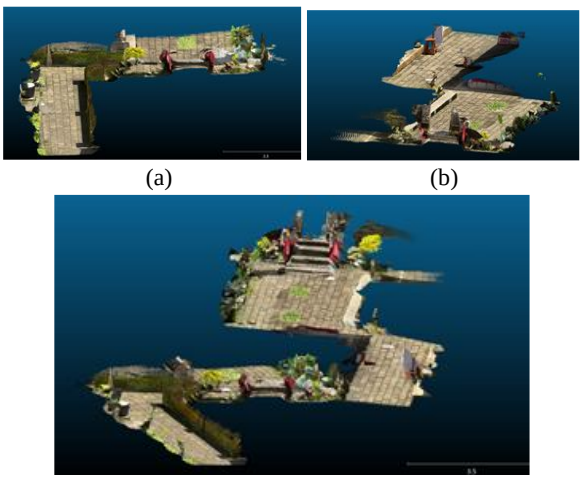

(a) (b)

(c)

Figure 5. (a). iPad LiDAR scan result of BGN5_A. (b). iPad LiDAR scan result of BGN5_B (c) Integration of BGN5_A and BGN5_B

4.4 Data Processing

4.4.1 Point Cloud Registration. Registration is carried out to combine point clouds from each lane. This study uses the cloud-to-cloud registration method. One of the algorithms commonly used in the cloud-to-cloud registration method is the Iterative Closest Point (ICP). This algorithm repeatedly matches points between the two point cloud data sets until achieving the optimal shape. Cloud-to-cloud registration requires parameters that must be set first. These parameters include the number of iterations, RMS difference, and overlap in the registration process. In this study, data processing was carried out by entering the expected RMS difference parameter of 2.0E-05 and an overlap of 30%.

The quality of cloud-to-cloud registration results using the ICP algorithm can be assessed by observing the registration results' Root Mean Square Error (RMSE) value. The smaller the RMSE value, the more accurate the registration process is, as in Table 2.

No	Point Clouds As references	Point Clouds to be registered	Over lap	RMS E
1	BGN5_A	BGN5_B	30%	0.0154 914
2	BGN5_B	MERGE (BGN5_C & BGN5_3)	30%	0.0277 991
3	MERGE (BGN5_C & BGN5_3)	MERGE (BGNJLN_3 & BGNJLN_5)	30%	0.0390 784
4	MERGE (BGNJLN_3 & BGNJLN_5)	MERGE JALAN (JLN_A s.d JLN_F)	30%	0.1580 37

Table 2. RMSE of cloud-to-cloud registration method with ICP Algorithm

Table 2 shows the quality of the registration results varies. This is due to various factors that affect the registration quality, such as the size of the overlap, the presence of noise, the presence of unpaired points, and the texture conditions of the scanned objects, which cause the RMSE value to be significant. For example, in registration no.4, the registration between the point clouds "MERGE (BGNJLN_3 & BGNJLN_5)" and MERGE JALAN (JLN_A to JLN_F) produces the most considerable RMSE value, which is 0.158 m. The significant result occurs because the overlap between the point clouds is less than optimal, and the lack of identical points is produced from the two overlapping point clouds. The condition of the point cloud is illustrated in Figure 6.

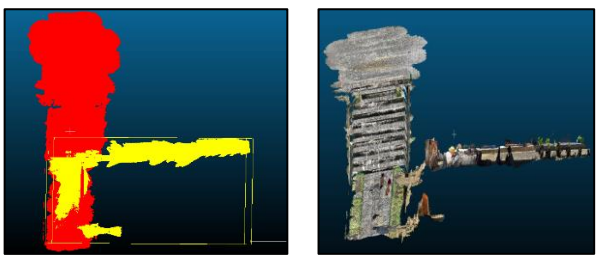

(a) (b)

Figure 6. (a) MERGE (BGNJLN_3 & BGNJLN_5) with MERGE JALAN (JLN_A s.d JLN_F). (b) registration result

4.4.2 Point Cloud Filtering. The point cloud filtering process removes noise or unwanted points from the point cloud data. Noise can come from various sources, such as imperfect data collection, environmental noise, or technical problems with the LiDAR device.

The more noise in the point cloud data, the more points will be removed during filtering. So, after the filtering process, the number of point clouds will be less than that of the original point clouds. The filtering process can be done automatically and manually. In this study, manual noise removal was carried out using the fencing technique. The noise removed is the buildings or objects above the ground that are still scanned when scanning. The removed objects are indicated by yellow arrows, as illustrated in Figure 7. The desired objects are only the ground surface, so the data that will be used for the next stage is point cloud data that describes the earth's surface model and can be processed into a raster as a DEM. The removed objects include terraced buildings, plants, and building walls.

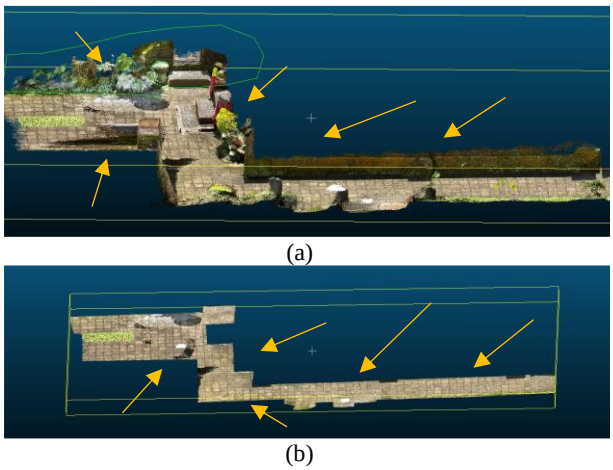

(a)

(b)

Figure 7. (a) Point cloud before filtering. (b) Point cloud after filtering.

4.5 Pont Cloud Georeferencing

The points used as point cloud references are GCP and ICP points. Before georeferencing, all registered LiDAR point cloud data are merged into one. The transformation process is carried out using the 7-parameter Helmert transformation method. The seven parameters include three translation parameters, three rotation parameters, and one scale factor. The transformation process is carried out using MATLAB software. The coordinate points on the point clouds are identified based on the placement of the marked GCP and ICP points, which will be used to transform the point cloud coordinates, which are still local coordinates, to UTM 50S projection coordinates from GNSS measurements using the static radial and real-time kinematic methods.

The number of point cloud points identified as common points in this Helmert transformation was selected as 31. The selection of control points must be evenly distributed in the scanned area so that the point cloud results do not experience shifting (tilting). Control points must be placed evenly at the scanned area's beginning, middle, and end to obtain good point cloud transformation results, as in Figure 8. This will ensure that the point clouds can be positioned accurately using the same coordinate system as the control points. From the results of the Helmert transformation, as shown in Table 3, it can be checked that there is a difference in coordinates in centimetre fractions between the reference coordinates in the form of UTM 50 S projection coordinates and the georeferencing results. This can occur because the ICP mark installed on the object's point cloud is not visible. This invisibility occurs during scanning, which causes the density of the point cloud to decrease.

Figure 8. Georeferenced point cloud data results

The RMSE value of the georeferenced results can be analysed during the transformation process. In georeferencing LiDAR data, RMSE is used to measure the accuracy of the coordinate transformation process.

Helmert Transformation Result Coordinates				
Point No	GCP/ICP	Easting (m)	Northing (m)	H. Ellips
Point#0	ICP30	319389.738	9068794.028	611.957
Point#1	GCPC	319388.553	9068797.868	612.011
Point#2	ICP29	319389.856	9068799.351	612.011
Point#3	ICP28	319386.686	9068800.397	612.072
Point#4	ICP27	319386.255	9068798.645	612.050
Point#5	ICP4	319384.099	9068805.368	612.508
Point#6	ICP26	319382.327	9068800.377	612.110
Point#7	GCPD	319380.199	9068798.301	612.078
Point#8	ICP1	319376.974	9068799.622	612.163
Point#9	ICP2	319375.111	9068799.815	612.171
Point#10	GCPB	319391.972	9068806.271	612.635
Point#11	ICP5	319380.519	9068809.569	612.656
Point#12	GCPA	319383.567	9068808.444	612.639
Point#13	ICP3	319369.316	9068802.299	611.876
Point#14	ICP25	319368.568	9068803.792	611.833
Point#16	ICP24	319370.883	9068810.470	612.005
Point#17	ICP21	319370.703	9068813.132	611.988
Point#18	ICP20	319373.675	9068814.562	612.325
Point#19	ICP19	319371.628	9068816.276	612.444
Point#20	ICP18	319374.323	9068816.416	612.842
Point#21	ICP17	319372.595	9068818.042	612.951
Point#22	ICP16	319375.194	9068818.077	613.307
Point#23	ICP15	319372.950	9068820.055	613.411
Point#24	ICP14	319375.958	9068820.227	613.814
Point#25	ICP13	319373.685	9068821.934	613.916
Point#26	ICP12	319376.037	9068822.037	614.278
Point#27	ICP6	319375.689	9068826.225	614.325
Point#28	ICP10	319376.314	9068824.081	614.325
Point#29	ICP11	319374.275	9068823.304	614.391
Point#30	ICP7	319374.471	9068828.269	614.310

Table 4. Georeferenced control point coordinates

The transformation process results at the georeferencing stage produced an RMSx value of 0.393 m, RMSy of 0.106 m, and RMSz of 0.553 m. The RMS of the elevation data had the highest results in the 55 cm fraction, and this was due to various reasons, one of which was that the iPad distance/height measurement was not carried out at the place where the scanning was carried out from the earth's surface, thus affecting the height accuracy. While the overall RMSE results obtained from the coordinate transformation were 0.687 m. Based on the RMSE produced, this value is relatively large, showing that the resulting accuracy is low or the accuracy of the point cloud data is in the tens of centimetres fraction when compared to the RMSE of the registration results, which are in cm units. This is caused by various factors related to the GCP's accuracy and the selection of objects to be transformed. The resulting DEM map can be equated to a map scale of 1:1.500 based on the error value.

The transformed data is obtained from the previously calculated parameters. These parameters include translation parameters to the x-axis, y-axis, and z-axis, rotation parameters to the x-axis, y-axis, and z-axis, and scale factors, as in Table 4. The scale factor is used as a multiplier for the rotation parameters.

Parameter	Result
X-Axis Translation	319381.9318
Y-Axis Translation	9068802.278
Z-Axis Translation	612.9590359
X-Axis Rotation	-0.015250295
Y-Axis Rotation	0.011510804
Z-Axis Rotation	-1.211479811
Scale Factor	0.986110005

Table 4. Transformation Parameter Results

The transformation of point cloud data is carried out iteratively according to the transformation parameters obtained through data processing using MATLAB, starting from translation, rotation, and scale. By obtaining the transformation parameter values, the point cloud georeferencing process can be carried out automatically from the initial local coordinates to UTM 50S projection coordinates. Figures 9 (a) and (b) are the results of point clouds that have been georeferenced.

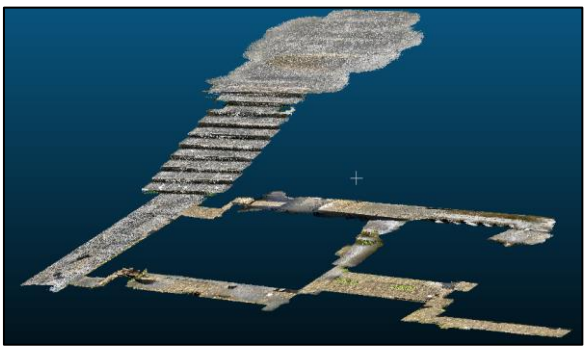

(a)

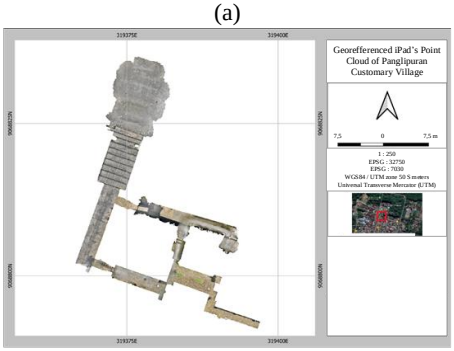

(b)

Figure 9. (a) Results of the Point Clouds Georeferencing Process (b). Map of the Results of the Georeferenced Point Clouds

4.6 DEM Generation

The grid method is used to create DEM. The processed DEM has been filtered and only consists of road topography data. Several parameters are used to develop DEM. The parameters used are grid size, projection direction using the z coordinate based on height, cell height using the average height value, and interpolation based on the average height value results. DEM formation is carried out on the iPad Pro M1 2021 LiDAR point cloud data. The DEM data is then compared with DEM data from

the photogrammetry method and the TLS method that already exists. A visualisation of the comparison of the three methods is shown in Figure 10.

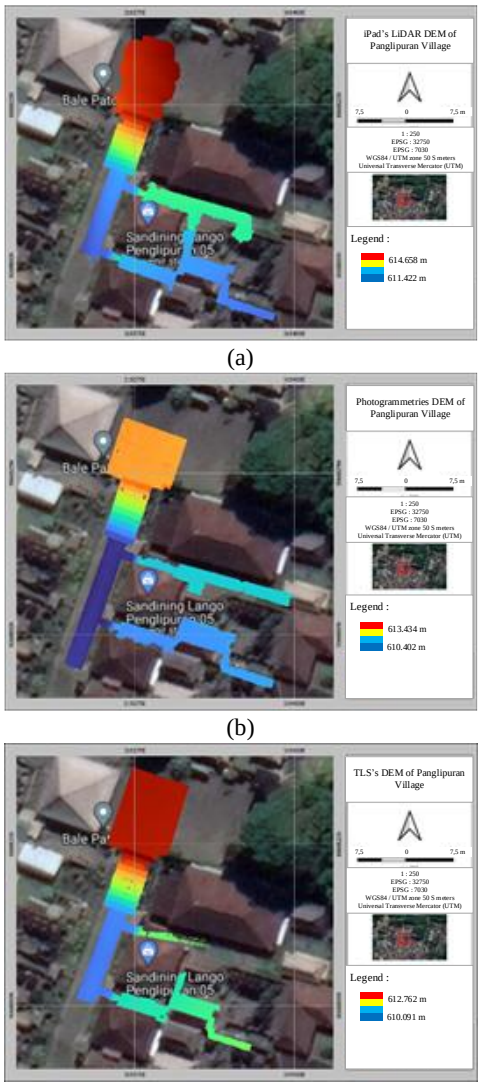

Figure 10. (a) DEM map from iPad LiDAR. (a) DEM map from Photogrammetry. (a) DEM map from TLS.

Figure 10 (a) shows the DEM visualisation generated from point cloud data using the iPad LiDAR method. The range of DEM elevation values in the research area is 611,422 m to 614,658 m. Figure 10 (b) is a DEM visualisation obtained using the close-range photogrammetry method in the same location, with an elevation range of 610,402 m to 613,434 m. The visualisation results shown in Figure 10 (c) are DEM visualisations from measurements using the TLS method with an elevation range of 610,091 m to 612,762 m. The DEM obtained with three different methods shows different height ranges. Photogrammetry and TLS methods have proven their accuracy in 3-dimensional mapping. They have better instrument settings than the iPad LiDAR, especially by using TLS, where the instrument is set in a static state, so the DEM data obtained from TLS is the best.

4.7 Customary Zone Definition

Based on the definition of the customary zone in Figure 1, the Utama mandala zone is located at the top and consists of holy places and temple buildings. The Madya mandala is a residential zone consisting of houses in the middle. The nista mandala zone consists of tombs. Based on local traditional beliefs, the zones are associated with the head, body and feet, where the utama zone is the head, the middle zone is the body, and the inferior zone is the feet. Based on visual analysis carried out on DEM and Point clouds data, it can be seen that the Utama zone is located in the upper temple road area, the Madya zone is the road area along the settlement towards the temple and the residential area, for the nista mandala zone which consists of tombs, no field data acquisition was carried out. The definition of customary zones is carried out by interpreting the division of customary zones using DEM data as illustrated in Figure 10 (a) and data from interviews with traditional leaders.

Customary Zone Elevation				Elevation Difference	
Utama Mandala		Madya Mandala		Utama Mandala	Madya Mandala
Min (m)	Max (m)	Min (m)	Max (m)		
614.066	614.658	611.422	614.571	0.592 m	3.149 m

Table 4. Definition of Customary Zones Based on Elevation

Customary definition of DEM data from georeferenced point cloud processing results, as in Table 4, can be visualised in 3D. 3D visualisation is done by displaying point cloud data from several viewpoints and paying attention to the orientation direction following the applicable customary policy that the spatial pattern in Penglipuran Village, Bali, is oriented towards Mount Batur in the north. The results of the 3D visualisation are used to create 3D maps using GIS software. The 3D map of customary zones is made based on integrating iPad LiDAR data with semantic data information regarding the division of customary zones, as in Figure 11 (a). 3D modelling is also carried out on shapefile data from defining customary zones, as in Figure 11 (b).

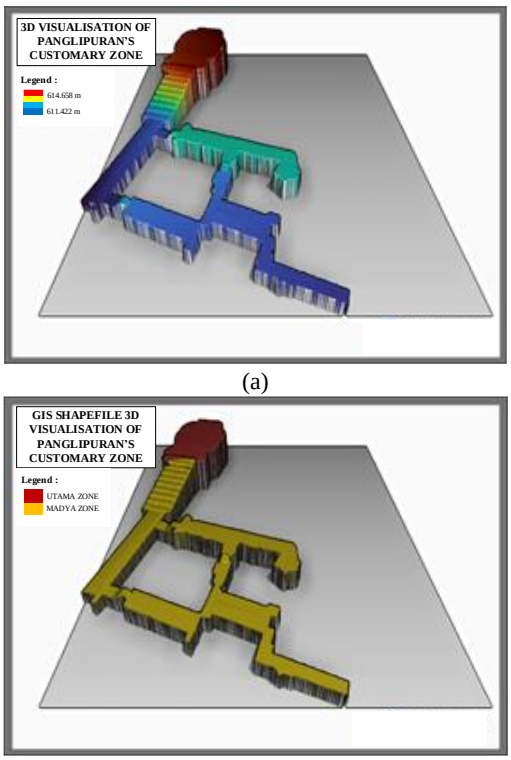

Figure 11. (a) 3D Modelling from DEM, (b) Shapefile customary definition zone.

5. Conclusion

The mechanism used to map 3D topography using LiDAR on the iPad Pro M1 2021 device must consider the design of the distribution of control points, both GCP and ICP. During scanning, attention must be paid to the overlap percentage between two adjacent lanes. The speed of the iPad movement during scanning also determines the number of points. The slower the scanning, the more point clouds result. Therefore, a scanning planning design is needed that considers the limits of the iPad LiDAR's capabilities. To obtain accurate results from transforming point clouds to the earth's coordinate system, the transformation must consider the datum parameters and projection system, including the distance from the iPad to the earth's surface, which will affect the elevation accuracy of the georeferenced point cloud.

The study's results show that the LiDAR sensor on the iPad device can be used to create 3D maps or A Digital Elevation Model (DEM) map. DEM maps in the study area can be produced according to the accuracy of the point cloud from the georeferencing process. Based on mapping standards in Indonesia, the resulting 3D or DEM maps can be equated with a 1: 1,500 scale map.

Adding information about customary rules inherent in 3D geometry can develop simple 3D visualisations in GIS models.

REFERENCES

Ariesta, K., Ariesta, K. S., & Ariastita, P. G. 2021. Pola Perubahan Penggunaan Lahan di Desa Tradisional Penglipuran Bali Berdasarkan Kondisi Faktual dan Persepsi Ruang Ketiga. *Jurnal Teknik ITS*, *9*(2), C14–C19.

Bobrowski, R.,Winczek, M.,Kulawik, K. Z., Węzyk, P. 2022. Best practices to use the iPad Pro LiDAR for some procedures of data acquisition in the urban forest. *Elsevier Urban Forestry & Urban Greening*, doi.org/10.1016/j.ufug.2022.127815.

Grant, D. S., 2013. Cloud To Cloud Registration For 3D Point Data. Dissertation of Doctor of Philosophy. Purdue University.

Gursel Y. Ç., Christopher J. P., Elena A. M. and Mark A. S. 2021. 3D LiDAR Scanning of Urban Forest Structure Using a Consumer Tablet. *MDPI, Urban Sci.* 2021, 5, 88. doi.org/10.3390/urbansci5040088.

Hakim, N. N. A., Razali, R., Said, M. S., Muhamad, M. A. H., Rahim A., H.1 and Mokhtar, M. A., 2023. Accuracy Assessment on Detail Survey Plan Using iPhone 13 Pro Max LiDAR Sensor. *International Journal of Geoinformatics, Vol.19, No. 5*. doi.org/10.52939/ijg.v19i5.2665.

Jacobs G (2005) Registration and Geo-referencing. Prof Surv Mag, July. leicageosystems.com/hds/en/ lgs_29445.htm

King, F., Kelly, R., & Fletcher, C. G. 2022. Evaluation of LiDAR-Derived Snow Depth Estimates From the iPhone 12 Pro. *IEEE Geoscience and Remote Sensing Letters*, *19*. doi.org/10.1109/LGRS.2022.3166665.

Lab˛ed´z P., Skabek, K., Ozimek P., Rola D., Ozimek A. and Ostrowska K. 2022. Accuracy Verification of Surface Models of Architectural Objects from the iPad LiDAR in the Context of Photogrammetry Methods. *MDPI, Sensors 2022, 22, 8504*. doi.org/10.3390/s22218504.

Li, Z., Zhu, Q., Gold, C., 2005. Digital Terrain Modelling-Principles and Methodology. CRC Press.

Luetzenburg, G., Kroon, A. and Bjørk, A. A., 2021. Evaluation of the Apple iPhone 12 Pro LiDAR for an Application in Geosciences. Scientific Reports-nature portofolio, doi.org/10.1038/s41598-021-01763-9.

Nelson, P., 2022. Evaluation of Handheld Apple iPad Lidar for Measurements of Topography and Geomorphic Change. agu2021fallmeeting-agu.ipostersessions.com/Default.aspx?s=86

Reshetyuk, Y., 2009. Self-calibration and direct georeferencing in terrestrial laser scanning. Doctoral thesis in Infrastructure, Geodesy. Doctoral thesis in Infrastructure, Geodesy.

Salleh, M. N., Mad Lazim, H. M., and Lamsali, H., 2018. Body measurement using 3D handheld scanner. *MoHE Movement, Health & Exercise*, 7(1), 179-187, 2018, *7*(1).

Saptari, A.Y., Widyastuti, R., Hamdani. 2022. Various High Density Point Clouds Registration Results Analysis in Heritage Building (Penataran Temple, Penglipuran Village, Bali). International Journal on Advanced Science, Engineering and Information Technology (IJASEIT) *12*(5).

Senapati, M,. Anand, B., Barsaiyan, V., and Rajalakshmi, P., 2020. Geo-referencing system for locating objects globally in LiDAR point cloud. 2020 IEEE 6th World Forum on Internet of Things (WF-IoT)

Spreafico, A.,Chiabrando, F., Losè, L. T., and Giulio Tonolo, F. 2021. *The iPad Pro Built-In LiDAR Sensor: 3D Rapid Mapping Tests and Quality Assesment. ISPRS Ann. Photogramm. Remote Sens. Spatial Inf. Sci.*,doi.org/10.5194/isprs-archives-XLIII-B1-2021-63-2021

Sudarwani, M. M. and Priyoga, I., 2018. A Study On Space Pattern and Tradional House Of Penglipuran Village. *Jurnal Ilmiah Arsitektur dan Lingkungan Binaan*, Vol 16, No.2, Oktober 2018; page 248-257

Teo, T. A., Yang, C. C. 2023. Evaluating the accuracy and quality of an iPad Pro's built-in lidar for 3D indoor mapping. *Elsevier Developments in the Built Environment* doi.org/10.1016/j.dibe.2023.100169.

Teppati Losè, L., Spreafico, A., Chiabrando, F., & Giulio Tonolo, F. 2022. Apple LiDAR Sensor for 3D Surveying: Tests and Results in the Cultural Heritage Domain. *Remote Sensing*, *14*(17). doi.org/10.3390/rs14174157

Voselmann,G., Mass, H.G., (2010). Airborne and Terrestrial Laser Scanning. CRC Press LLC, Taylor and Francis Group.

Wahyudi Arimbawa, B.-B., & Komang Gede Santhyasa, I. 2017. Perspektif uang Sebagai Entitas Budaya Lokal. Orientasi Simbolik Rung Masyarakat Tradisional Desa Adat Penglipuran, Bangli-Bali. *Local Wisdom : Jurnal Ilmiah Kajian Kearifan Lokal*, *2*(4), 01–09.